Cold Fusion Reactions with ^{48}Ca

H.W. Gäggeler, D.T. Jost
Paul Scherrer Institute, CH-5232 Villigen Switzerland
A. Türler
Laboratorium für Radiochemie, Universität Bern, CH-3000 Bern, Switzerland
P. Armbruster, W. Brüchle, H. Folger, F.P. Hessberger, S. Hofmann, G. Münzenberg, V. Ninov, W. Reisdorf, M. Schädel, K. Sümmerer
Gesellschaft für Schwerionenforschung bmH, D-61 Darmstadt, Fed.Rep.of Germany
J.V. Kratz, U. Scherer
Institut für Kernchemie, Universität Mainz, D-65 Mainz, Fed.Rep. of Germany
M.E. Leino
Department of Physics, University of Helsinki, Finland

Fusion reactions of ^{48}Ca projectiles with ^{180}Hf, ^{184}W, ^{197}Au, ^{208}Pb and ^{209}Bi were studied. All experiments were performed at the SHIP velocity filter. As target 300 to 400 µg/cm^2 thick metallic foils were used which were either mounted on a rotating target wheel (^{208}Pb, ^{209}Bi, ^{197}Au) or used as single targets (^{180}Hf, ^{184}W). Evaporation residues were detected via their α-decay. In case of the reaction with ^{208}Pb evaporation residues from the 1n and 2n channel were also detected via their grand-daughter nuclides using chemical techniques[1].

All results are summarized in the Table 1[2]. For the heavier systems ^{197}Au, ^{108}Pb and ^{209}Bi the data can be well reproduced with the code HIVAP assuming no (or only a small) hindrance of fusion, i.e. Extra-Extra-push $E_{XX} \leq 5$ MeV. Fig. 1 summarizes (E_{XX}) values from the literature and from this work.

Surprisingly, for the lighter systems (^{180}Hf, ^{184}W) the measured cross sections (3n-channel) were more than two orders of magnitude smaller than expected (HIVAP). At present we have no explanation for this discrepancy. Agreement between experimental and calculated values can only be obtained by reducing the macroscopic fission barries of the compound nuclei by 30 to 40 %. Fig. 2 depicts a schematic of how evaporation residue cross sections evolve for compound nuclei between Th and Lr.

[1] H. Gäggeler et al. GSI-scientific report 1988, GSI-89-1, p.18.
[2] H. Gäggeler et al. Nucl.Phys. A502, 561c (1989).

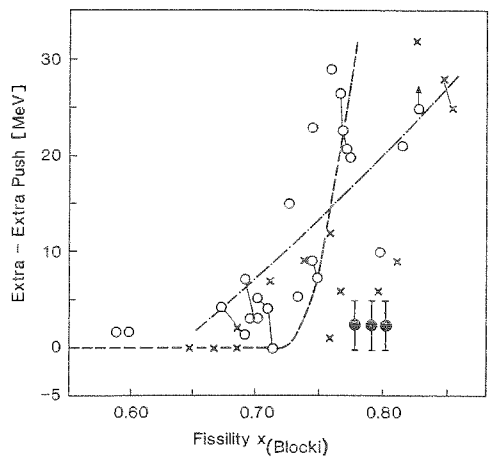

Fig. 1: Extra - extra push values from the literature (open circles and crosses) and from this work (closed circles) as a function of the fissility parameter[12].

Table 1: Experimental cross sections

Reaction	Incident Energy [MeV/u]	Excitation Energy[a] [MeV]	1n [nb]	2n [nb]	3n [nb]
$^{48}Ca + ^{208}Pb$	4.34	13.2	≤ 27	≤ 27	
	4.42	16.3		212 ± 58	
	4.42[b]	16.7	260 ± 30	420 ± 50	
	4.44[b]	17.4		730 ± 150	
	4.50	19.3		2344 ± 544	
	4.50[b]	19.7	180 ± 53	3385 ± 310	
	4.50[b]	19.7		3110 ± 480	
	4.57	21.9		1845 ± 435	
	4.65	25.2		418 ± 114	$37 \pm {}^{34}_{20}$
	4.74	28.8		39 ± 19	109 ± 33
$^{48}Ca + ^{209}Bi$	4.38	13.7	≤ 4.5		
	4.46	17.6	61 ± 20	12 ± 7	
	4.53	19.6	20 ± 11	437 ± 96	
	4.61	22.7	≤ 7.5	324 ± 75	
	4.69	25.8		38 ± 11	9 ± 5
	4.76	29.4			28 ± 11
$^{48}Ca + ^{197}Au$[c]	4.42	27.6		40 ± 15	
	4.48	30.0		42 ± 17	
	4.63	35.6		36 ± 15	
$^{48}Ca + ^{184}W$	4.20	34.4			$4 \pm {}^{10}_{4}$
$^{48}Ca + ^{180}Hf$	4.24	36.0			128 ± 59

[a] In the middle of the target (chemistry) or at 2/3 of the target (SHIP). Energy width within target ± 1.2 MeV (chem.) and $\pm {}^{1.6}_{0.8}$ MeV (SHIP). Additional energy uncertainty from UNILAC ± 0.8 MeV.
[b] Results from chemisty, all other data from SHIP.
[c] Sum of 2n and 3n channel (see text).

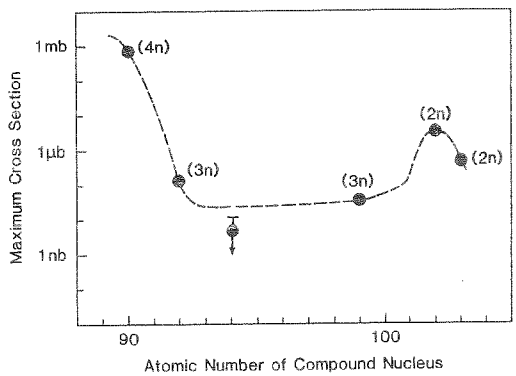

Fig. 2: Maximum cross sections for the main xn channels from ^{48}Ca induced fusion reactions.

Reactions of ^{40}Ar with ^{233}U, ^{235}U, and ^{238}U at the Barrier[B]

U.W. Scherer[1], W. Brüchle[2], M. Brügger[2], C. Frink[1], H. Gäggeler[3], G. Herrmann[1,2], J.V. Kratz[1], K.J. Moody[2,*], M. Schädel[2], K. Sümmerer[2], N. Trautmann[1], G. Wirth[2]

[1]Institut für Kernchemie, Universität Mainz
[2]Gesellschaft für Schwerionenforschung mbH, Darmstadt,
[3]Paul Scherrer Institut, Villigen, Switzerland

The reactions of ^{40}Ar with $^{233,235,238}U$ were investigated at the Coulomb barrier by measuring cross sections for target-like reaction products. The heaviest products detected are isotopes of californium (Z=98). In addition to the quasi-elastic component in the isotopic distributions observed in the vicinity of uranium, there are also relaxed contributions throughout the entire region. For this component, the element yields below uranium are the same within the error limits for the three target isotopes; the yields above the target are higher for ^{238}U than for ^{235}U and lowest for ^{233}U. It is suggested that these trends reflect the gradients of the potential energy surfaces for the three reactions.

As to the centroids of the isotopic distributions at a given value of Z, we find that these, after the transfer of >3 charges, approach closely the minimum of the potential energy valley. This is depicted for $^{40}Ar+^{235}U$ in Fig. 1, where open symbols stand for a bombarding energy $E/E_B=1.0$, and closed symbols for $E/E_B=0.97$. The centroids for the trans-target products coincide at both incident energies; below the target the products seem to be slightly more neutron-rich at the lower-bombarding energy even though this is barely outside the uncertainty limits. In addition to the equi-potential lines, Fig. 1 contains two bold solid lines to the left of the dotted minimum potential energy (MPE) line. These indicate the expected location of the centroids of the post-neutron emission isotope distributions under the assumption of an excitation energy sharing in proportion with the fragment masses. The bold solid line closer to the MPE line is based on the assumption of an exit channel barrier for two touching spheres, whereas the bold solid line further to the left is based on the assumption of Viola kinetic energies. Neither assumption reproduces correctly the observed centroids. For the trans-target products the predicted product locations approach the MPE line for trivial reasons. This is because the Q_{gg} values become increasingly negative (-50 MeV for Cf) with increasing product Z, and the excitation energies become very small. We have to conclude that the experimental data are in conflict with a sharing of the total excitation energy in proportion to the masses, at least for the below-target products, which seem to be much less excited than expected.

This is reminiscent of similar observations in the Ca+Cm reactions[1,2], and in reactions of ^{50}Ti, ^{54}Cr, and ^{58}Fe with Pb[3] at the barrier. In the latter cases, it was found that the projectile-like acceptors of the transferred nucleons carry essentially all of the excitation energy, and the target-like donors stay cold. The condition for this "unusual" excitation energy sharing are the same in the present work and in Refs. I-3: The bombarding energy corresponds exactly to the Coulomb barrier so that the velocity of the relative motion is zero at contact. Thus, there is no initial friction force and the transfer of nucleons may occur frictionless.

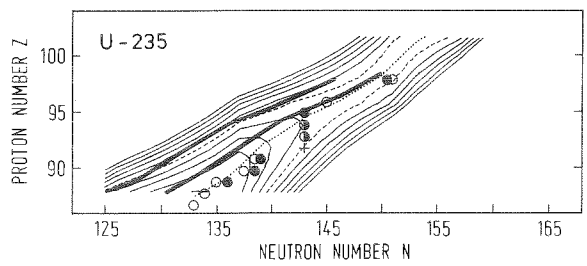

Fig.1 Potential energy surface for $^{40}Ar+^{235}U$. The open and closed dots indicate the locations of the centroids of the experimental isotopic distributions. The bold solid lines are expectations for these locations, see text.

[1] H. Gäggeler et al., Phys. Rev. C33, 1983 (1986)
[2] A. Türler, Doctoral Thesis, University of Bern, 1989
[3] H. Keller et al., Z. Phys. A328, 255 (1987)

1n-Transfer Reactions in Collisions of U + Au and Au + Au near the Coulomb Barrier[B]

G. Wirth, W. Brüchle, Fan Wo, E. Jäger and K. Sümmerer
GSI Darmstadt
F. Funke, J.V. Kratz, and N. Trautmann
Institut für Kernchemie, Universität Mainz

We have investigated nuclear reactions in the collisions of very heavy ions at energies near and below the Coulomb barrier over the last years. One-neutron transfer turned out to be the most probable direct reaction[1]. The excitation function of the 1n-transfer product ^{239}U in the reaction ^{238}U + ^{238}U could be well reproduced by a simple semiclassical Sub-Coulomb transfer theory whereas the angular distributions in the same reaction revealed large discrepancies between experiment and theory for the more central collisions. Sequential fission after 1n-transfer did not provide an explanation[2]. Therefore we extended the 1n-transfer measurements to the systems U + Au and Au + Au in order to study possible influences of the static deformation of the collision partners and of the symmetry of the system ("Pauli-Blocking") on the angular distributions.

Since the 1n-transfer measurements in the asymmetric system U + Au were designed to search for deviations from Rutherford trajectories[3] in the same experiments, irradiations were performed at 15 incident energies around the Coulomb barrier yielding a very large number of cross sections for the 1n-transfer products ^{198g}Au, ^{196g}Au and also their isomeric states ^{198m}Au and $^{196m2}Au$. Fig. 1 shows the transfer probabilities versus the reduced distance of closest approach for the 1n-transfer product ^{198g}Au in the reaction ^{238}U + ^{197}Au. The data are in excellent agreement with the semiclassical theory over 4 orders of magnitude. The slope parameter of the linear fit (1.08 ± 0.02 fm^{-1}) agrees very well with the value expected from neutron binding energies (1.10 fm^{-1}). On the other hand, in the same reaction ^{238}U + ^{197}Au the angular distributions of the 1n-stripping transfer product ^{196g}Au show large deviations from the semiclassical theory. This is demonstrated in fig. 2 displaying various angular distributions at the same energy relative to the Coulomb barrier. Similar deviations from the theory are obtained from the analysis of the cross sections of the isomeric states ^{198m}Au and $^{196m2}Au$. In the symmetric reaction ^{197}Au + ^{197}Au we measured angular distributions for the already mentioned 1n-transfer products at four energies below the barrier. In all cases the angular distributions of the 1n-transfer products are not in agreement with the semiclassical theory. Similar to the ^{238}U + ^{238}U data and most of the ^{238}U + ^{197}Au data, the theory fits only to the more peripheral collisions as demonstrated in fig. 2c. It should be noted that the data for the symmetric Au + Au-system have been reduced in a similar way as described in ref. 2 for comparisons to unsymmetrized calculations.

To summarize our experimental 1n-transfer results in very heavy ion collisions at low energies, we find that the ^{198g}Au differential cross sections in the reaction ^{238}U + ^{197}Au are the only data that are in complete agreement with the semiclassical theory for all scattering angles excluding the region of trivial absorption. Effects from the static deformation of the collision partners are not observed in the angular distributions, because the 1n-stripping channel in the ^{238}U + ^{197}Au system agrees with the theory whereas the complementary 1n-pickup channel does not. In addition, the much less deformed ^{197}Au + ^{197}Au system shows deviations from the theory for the central collisions which are comparable with those observed in ^{238}U + ^{238}U and most ^{238}U + ^{197}Au angular distributions. Pauli-Blocking too seems not to be that important because of the deviations in the angular distributions of most 1n-transfer products in the asymmetric ^{238}U + ^{197}Au system.

An interesting correlation of the observed deviations is found with the ground state Q-values (the reaction Q-values were not measured) of the various reactions. ^{198g}Au in the system ^{238}U + ^{197}Au is the only 1n-transfer product with a positive ground state Q-value and at the same time the only 1n-transfer product that is in agreement with the theory at all angles.

1. G. Wirth et al., Phys. Lett. **B177**(1986)282
2. G. Wirth et al., Z. Phys. **A330**(1988)87
3. G. Wirth et al. in: Heavy Ion Interactions Around the Coulomb Barrier, Springer 1988, p. 84

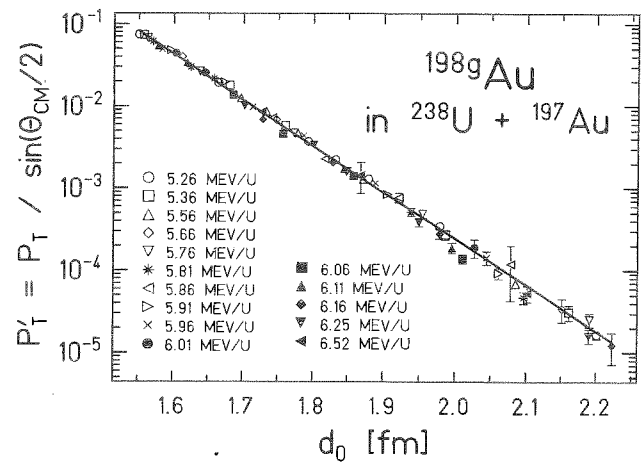

Fig. 1: Transfer probabilities for ^{198g}Au in the reaction ^{238}U + ^{197}Au. The line is a two-parameter fit of the semiclassical theory to the data. Only data with $d_0 > 1.55$ fm are shown.

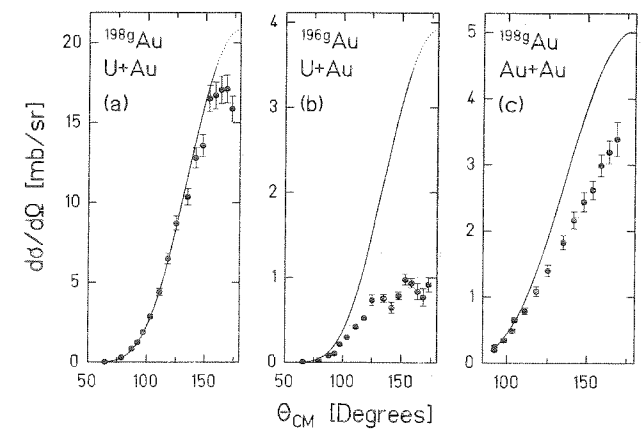

Fig. 2: Angular distributions of 1n-transfer products at 88% of the Coulomb barrier. The lines are fits of the semiclassical theory. The region where absorption, not considered in the theory, sets in ($d_0 < 1.55$ fm), is indicated by a dotted line.

Multi-Nucleon Transfer in U+U and U+Au Collisions [B] below and near the Coulomb Barrier

F. Funke, J.V. Kratz, N. Trautmann
Institut für Kernchemie, Universität Mainz
G. Wirth, W. Brüchle, Fan Wo, E. Jäger, K. Sümmerer
GSI Darmstadt

We have previously reported on the fission excitation function[1] in the U+U reaction. The high fission cross sections exceeding the expected cross sections for Coulomb fission for bombarding energies >0.9xV_c were tentatively attributed to sequential fission following multi-nucleon transfer. The finite fission widths associated with the decay of such multinucleon transfer products requires, for consistency, the observation of surviving products from the transfer of many nucleons. We have measured excitation functions for the formation of several radiochemically accessible Ra, Ac, Th, and Pa isotopes. The excitation functions[2] were found to be very similar to each other suggesting that these isotopes are members of a broad product distribution which is similar in both reactions U+U and U+Au. It has been suggested that these products originate from a small fraction of collisions in which, due to the deformation of one or both collision partners, nuclear contact and the onset of neck formation are established even well below the spherical Coulomb barrier.

Meanwhile, we have studied the systematics of isotope yields for the elements Ra through Pa in both reactions and have arrived at the following conclusions: the yields, see Fig. 1, are consistent with the usual Gaussian systematics and have widths of FWHM≈ 2.8 mass units. The centroids of these Gaussians coincide within the uncertainties with the minimum potential energy (MPE) prediciton, and the position of the centroids does not change with the bombarding energy. These observations suggest that these products have been formed cold, so that neutron evaporation/fission did not play a significant role in their production process. This is consistent with similar results in the $^{40}Ar+^{233}U$, ^{235}U, ^{238}U reactions[3], in reactions of ^{50}Ti, ^{54}Cr, ^{58}Fe with Pb[4], and in the $^{48}Ca+^{248}Cm$ reaction[5]. In all these reactions, as in the present work, the bombarding energy was at (or below) the Coulomb barrier. Thus, the present data add to the conjecture that the donors of the transferred nucleons stay cold and the acceptors carry most of the excitation energy[4], if the collision occurs with relative velocity zero.

From the integrals of the isotopic distributions together with interpolations and extrapolations based on the Wollersheim systematics[6] with parameters adjusted[7] to reproduce the energy dependence of the below-target element yields above the barrier in the U+U reaction[8] we obtain an integral cross section for the surviving below-target multi-nucleon transfer products of 15 mb both for the U+Au and U+U reaction at the barrier. The cross section for sequential fission[1] in the U+U reaction is 100 mb. If we assume that all the heavy complements of the below-target multinucleon transfer products decay by sequential fission, at most 15 mb can be contributed to the sequential fission cross section by multi-nucleon transfer. Fission after 1n-transfer[1] contributes 5 mb. Thus, we have to conclude that the majority of sequential fission processes must occur after the transfer of a few nucleons, i.e. in transfer channels intermediate between one-nucleon and multi-nucleon transfer, for which sufficient cross section should exist. The surviving part of this cross section was not accessible to the radiochemical method.

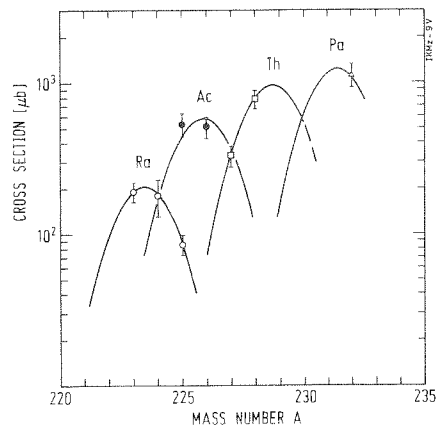

Fig.1 Cross sections for multi-nucleon transfer products in the U+Au reaction at the barrier

[1] G. Wirth et al., Z. Phys. A330, 87 (1988)
[2] G. Wirth et al., GSI Scientific Report 1988, GSI-89-1, p.41
[3] U.W. Scherer et al., Preprint GSI-89-85 (1989) Z. Phys. A, in press
[4] H. Keller et al., Z. Phys A328, 255 (1987)
[5] H. Gäggeler et al., Phys. Rev. C33, 1983 (1986)
[6] H.J. Wollersheim, Report GSI-84-34 (1984)
[7] H. Gäggeler, PSI-Bericht Nr. 14 (1988)
[8] J.V. Kratz et al., GSI Scientific Report 1979, GSI-80-1, p.27

Development of fast α-HIB Separations of Element 105 [B]

H.P. Zimmermann[1], W. Brüchle[2], M.K. Gober[1], J.V. Kratz[1], M. Schädel[2], N. Trautmann[1]

[1] Institut für Kernchemie, Universität Mainz

[2] GSI, Darmstadt

In 1988 we have studied the halide complex formation of element 105 in aqueous solutions by anion exchange separations of 34-s $^{262}_{105}$Ha relative to its homologues niobium and tantalum, and to protactinium [1]. Also, volatile bromides of $^{262}_{105}$Ha have been prepared and separated by isothermal gaschromatography [2].

In the latter experiments evidence was found for the existence of a $\sim$ 10 -s spontaneous fission (SF) activity which might be another isomer or isotope of element 105, possibly the hitherto unknown $^{263}_{105}$Ha. This activity could not be detected in the anion exchange separations because assay of the samples for α-particle and SF activity did not start before 55 s after the end of bombardment.

In order to verify the existence of such a short-lived SF activity, much faster aqueous-phase separations of element 105 and a much faster procedure for sample preparation have to be developed. To this end, we have studied elutions of pentavalent, tetravalent and trivalent metal ions from cation exchange columns in unbuffered solutions of α-hydroxy-iso-butyric acid (α-HIB). α-HIB complexes of the pentavalent group-V elements should immediately be eluted from the resin, while the interferring tetravalent group-IV elements are retained on the column. This is even more the case for the trivalent actinides. Besides providing a faster access to element 105, the method is expected to provide also an independent proof of the 5+ oxidation state of element 105 in aqueous solution, and an improved decontamination from the interferring actinides.

We have manually performed HPLC separations using the cation exchange resin Aminex A6 (particle size $17.5 \pm 2\mu m$) and tracer activities of ^{95}Zr, ^{95}Nb and ^{233}Pa produced at the Mainz TRIGA reactor. The activities were dissolved and stored in unbuffered solutions of various α-HIB concentrations. The columns (1.7×25 mm) were prewashed with solutions of the same α-HIB concentration. The tracer activities were fed onto the columns through a sample loop. Fig.1 shows the elution behaviour of the pentavalent Nb and Pa from the column in 0.075 M α-HIB at a flow rate of 1 ml/min. After the dead volume of about 130 μl ($\sim$ 7s), both activities appear in the effluent and are eluted completely within another $\sim$ 150 μl ($\sim$ 9s). The first activity of the tetravalent Zr is detected after the elution of another 3150 μl ($\sim$ 190 s). By increasing the α-HIB concentration to 0.5 M, zirconium, after the elution of Nb and Pa in 0.075 M α-HIB, can be eluted in 210 μl ($\sim$ 12 s), see Fig.1.

This separation is presently being implemented at the Automatic Rapid Chemistry Apparatus, ARCA II [3], which, itself, was subject to major mechanical improvements. First experiments were performed on the tantalum isotopes $^{168-170}$Ta produced on-line at the UNILAC accelerator, and transported by a He/KCl gas-jet transportation system to ARCA II, where they were deposited on a polyethylene frit. The dissolution of the collected tantalum activity from the frit was investigated as a function of the α-HIB concentration. Because of the smaller column size in ARCA II (1.6 x 8 mm) which might cause an earlier breakthrough of the tetravalent and trivalent metal ions it was desirable to decrease the α-HIB concentration. Even with 34 μl of 0.025 M α-HIB, dissolution of > 75 % of the collected tantalum activity was achieved within 2 s. Due to the smaller column size and to the smaller dead volume of 35 μl, the time required for the complete separation of the element 105 fraction is anticipated to be of the order of a few seconds.

In order to avoid the time consuming preparation of weightless samples for α- and SF counting by evaporation to dryness, the effluent will be eluted directly onto the surface of a large area passivated implanted planar silicon (PIPS) detector as a thin layer ($\sim$ 20 μm). Under these conditions, an energy resolution of FWHM $\simeq$ 40 keV at E_α = 8.8 MeV can be achieved [4].

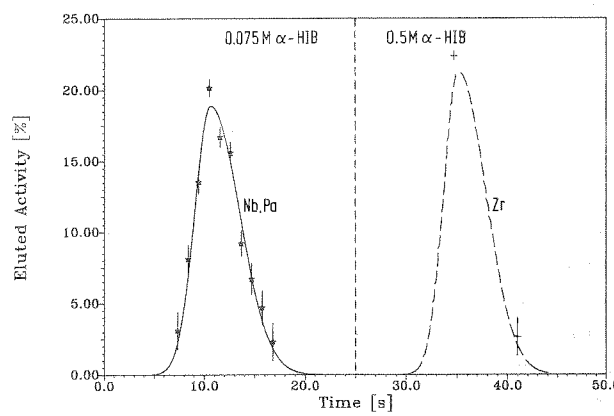

Figure 1.: Elution of Nb and Pa in 0.075 M α-HIB from a 1.7 x 25 mm cation exchange column, followed by the elution of Zr in 0.5 M α-HIB.

[1] J.V. Kratz et al., Radiochim. Acta, 48,121(1989)
[2] H. Gäggeler et al., PSI-Report Nr. 49 (1989)
[3] M. Schädel et al., Radiochim. Acta, 48,171(1989)
[4] F. Haberberger, Diploma Thesis, Mainz (1989)

Gaschemical separations by selective desorption from small KCl particles

A. Türler

Lawrence Berkeley Laboratory, Berkeley, CA

D.T. Jost, H.W. Gäggeler, A. Kovacs

Paul Scherrer Institut, Villigen, Switzerland

W. Brüchle, H. Folger, M.Schädel

GSI - Darmstadt

M. Gober, J.V. Kratz, P. Zimmermann

Institut für Kernchemie, Universität Mainz

For chemical studies of heaviest elements on-line separations in the gas-phase have proven to be very useful and fast. In recent years this technique was applied to search for superheavy elements[1] and to study chemical properties of the heavy elements Lr[2] and 105[3].

So far, the nuclides of interest were transported to the gaschemistry set-up by a gas-jet device, mostly using KCl as transporting species. In the chromatography column (usually quartz or metal) the particles containing the reaction products were stopped on a wool plug which was heated to a fixed temperature of about 1000 to 1100 ^{0}C. Volatile species evaporating from this collecting plug were then separated in a following isothermal section of the oven. Depending on the temperature of this section species of a certain volatility were passing the chromatography column and were then available for counting. For a detailed description of the entire chromatography apparatus see[2,4]. The advantage of this technique is its speed and continuous mode which allows chemical separations within a few seconds[4]. The disadvantage, however, are the rather poor chemical separation factors. Therefore, this technique was applied so far only for separations of groups of elements (as atoms or molecules) with distinctly different volatilities, e.g. in separations of highly volatile trans-actinide halides from the much less volatile actinides halides[3].

In the following we have tried to perform chemical separations using the same gaschromatography device but varying the temperature of desorption of the products from the transporting KCl particles.

A 12.5 mg/cm^2 thick La target, mounted behind a double window system of 3.4 mg/cm^2 Mo and 2 mg/cm^2 Be, was bombarded with ^{40}Ar projectiles of an incident energy of 9.2 MeV/u. This defines an energy range within the target of 8.10 to 6.26 MeV/u. According to a HIVAP calculation for this energy range mainly nuclides from the channels 7n, p7n and α4n to α7n should be produced, all with cross sections above 10 mb.

In the following we have analysed only such nuclides which are mainly produced directly, such as ^{172B}Re ($T_{1/2}$ = 15 s), ^{170}W (2.4 min) or ^{166}Ta (32 s). In addition, we also included into our chemical study ^{99m}Nb which was studied at PSI with the same set-up using its production via fission of ^{235}U at the SAPHIR reactor[4].

For all the above mentioned nuclides the desorption behaviour from small (Ø ≈ 40 nm) KCl particles was studied which were collected on a quartz wool plug. HBr and HCl were used as reactive gas. Typical gas-flow rates were 1 l/min of carrier gas (He) and 100 ml/min of reactive gas which was added to the carrier gas at the postion of the wool plug. The temperature of the isothermal part of the oven was kept at 500 ^{0}C and 600 ^{0}C, respectively, for HBr and HCl. After the column the products were thermalized, attached onto new KCl aerosols and transported along a capillary to a collecting glass fibre filter, mounted on top of a HPGe detector for γ-spectroscopy (for details see[2]).

Fig. 1 shows the result with HBr as reactive gas. 100 % desorption yield represents the maximum value of the chemical yield, which is dependent on the half-life of the nuclide[4]. Typical values for the *absolute* chemical yields are 70 % for ^{170}W and 20 % for ^{172B}Re. Easiest desorption is obtained for Re, followed by W, Nb and Ta. This sequence may be explained by the maximum oxidation states of the corresponding elements. In case of Nb and Ta, both transition elements from group V, easier desorption is observed for Nb as compared to Ta, in agreement with results from isothermal chromatography[3].

With HCl the desorption temperatures are higher than with HBr. This can be explained by a lower volatility of chlorides compared to bromides. Fig. 2 shows, as an example, the data for ^{166}Ta with HBr and HCl. Surprisingly, the desorption curve measured with HCl has a local minimum at about 750 ^{0}C. We attribute this minimum to a melting of the KCl particles (melting point 760 ^{0}C).

[1] P. Armbruster et al., Phys.Rev.Lett., *54*,406(1985)

[2] D.T. Jost et al., Inorg.Chim.Acta *146*, 255(1988)

[3] H.W. Gäggeler et al., Report PSI-49(1989)

[4] Ya Nai-Qi et al., Radiochim.Acta, *47*,1(1989)

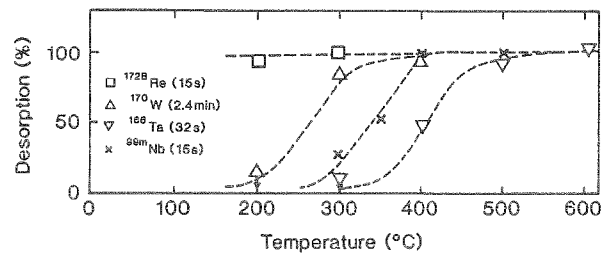

Fig.1 : Relative desorption yields for some elements from KCl particles with HBr as reactive gas.

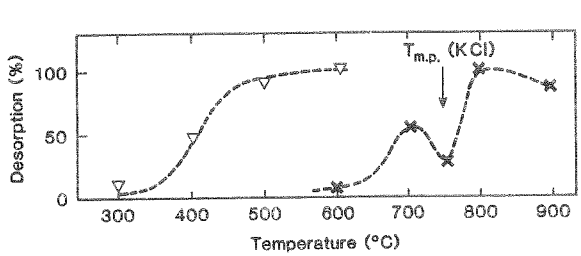

Fig.2: Relative desorption yields for ^{166}Ta from KCl with HBr (triangles) and HCl (crosses).

Chemical Separation of Transfer Products in the Reaction $^{22}Ne + ^{238}U$

M.K. Gober[1], J.V. Kratz[1,2], U.W. Scherer[3], H.P. Zimmermann[1], W. Brüchle[2], M. Schädel[2], B. Schausten[2]

[1]Institut für Kernchemie der Universität Mainz

[2]Gesellschaft für Schwerionenforschung, Darmstadt

[3] presently at Paul Scherrer-Institut, CH-5303 Würenlingen

A chemical separation procedure for the isolation of reaction products with $88 \leq Z \leq 100$ was developed to determine their production cross sections in the reaction of ^{22}Ne with ^{238}U at bombarding energies of 112 resp. 122 MeV. It was also planned to measure the transmission of ^{252}Fm through the gas filled seperator NASE. ^{252}Fm is generated in two different reaction channels:

$$^{238}U\ (^{22}Ne,\ 4n)\ ^{256}No \longrightarrow\ ^{252}Fm$$
$$^{238}U\ (^{22}Ne,\ \alpha 4n)\ ^{252}Fm$$

The excitation function for the 4n-reaction has its maximum at 112MeV and a cross section of 43nb whereas the α4n-reaction has a maximum cross section around 122MeV, while at 112MeV there is $\sigma \approx$ 50nb [1]. Moreover, there is a possibility, that ^{252}Fm is formed in transfer reactions, so that the determination of the systematics of transfer cross sections of heavy target-like reaction products is of considerable interest.

The chemical procedure is based on the one developed by Scherer for the separation of the Actinides and Ra in the $^{40}Ar + ^{233,235,238}U$ reactions. Chemical yields and purity of the different fractions were monitored by radioactive tracers chemically similar to the different elements, except for the light actinides where the yields of two previous tracer experiments where assumed, because most of the potential tracer isotopes were expected to be main reaction products.

In the experiment, a $^{238}UF_4$-target (290μg $^{238}U/cm^2$) on a 39μg carbon backing was irradiated with $^{22}Ne^{8+}$ at 500 pnA. The reaction products were collected in a Ni-catcher foil situated behind the target. Unfortunately, in the first experiment, the target was heavily damaged and partly detached from the target wheel, so that it is not possible to obtain absolute cross sections.

After the end of bombardment the catcher foil was dissolved in concentrated HNO_3, tracers and carriers were added and chemical processing was carried out. The chemical yields of the different steps were between 80 and 99%, except for the $BaCO_3$-Precipitation (30%).

Before the final samples were prepared for counting, the Transplutonium elements (TPE) were cleaned up by means of small cation-exchange columns, with an average chemical yield of 85%. Afterwards, they were electroplated on Ti-disks. The yield of electrodeposition was determined by addition of ^{177g}Lu-tracer, it was around 93%.

Pu and Th were electroplated on Ti-discs, too, but with relatively poor yields compared to the heavy actinides (Pu 70%, Th 60%).

Ra and Ac were eluted together from the HDEHP-column, the fraction was evaporated to dryness on a Ta-disc, γ-counting of the ^{133}Ba gave a yield of 100% in this step.

The samples for γ-counting (Pa - Np, Bk) were prepared by co-precipitation with $Fe(OH)_3$ as carrier and ^{177g}Lu as tracer (quantitative).

The overall chemical yields for all elements after clean-up and sample preparation are shown in the table below. Tracer isotopes and yields designated by a * are from tracer experiments.

We observed no cross contaminations due to incomplete separation. The chemical yields of Ba, Th, Pu and of the heavy actinides are still being optimized.

The fusion evaporation residue 25.4h-^{252}Fm was clearly identified by its 7.04 and 7.0MeV α-radiation. Production rates relative to the ^{252}Fm production rate of target-like transfer-products are being determined.

Element	Tracer	yield	Element	Tracer	yield
Ra	^{133}Ba	26%	Am	^{147}Nd	59%
Ac	^{140}La	85%	Cm	^{151}Pm	66%
Th	$^{230}Th^*$	48% *	Bk	^{152g}Eu	66%
Pa	$^{233}Pa^*$	80% *	Cf	^{153}Gd	53%
U	^{233}U *	80% *	Es	^{160}Tb	72%
Np	$^{237}Np^*$	80% *	Fm	^{86}Y	53%
Pu	$^{238}Pu^*$	56% *			

[1] E.D. Donets et al, Atomnaya Energiya *16*, 195 (1964)

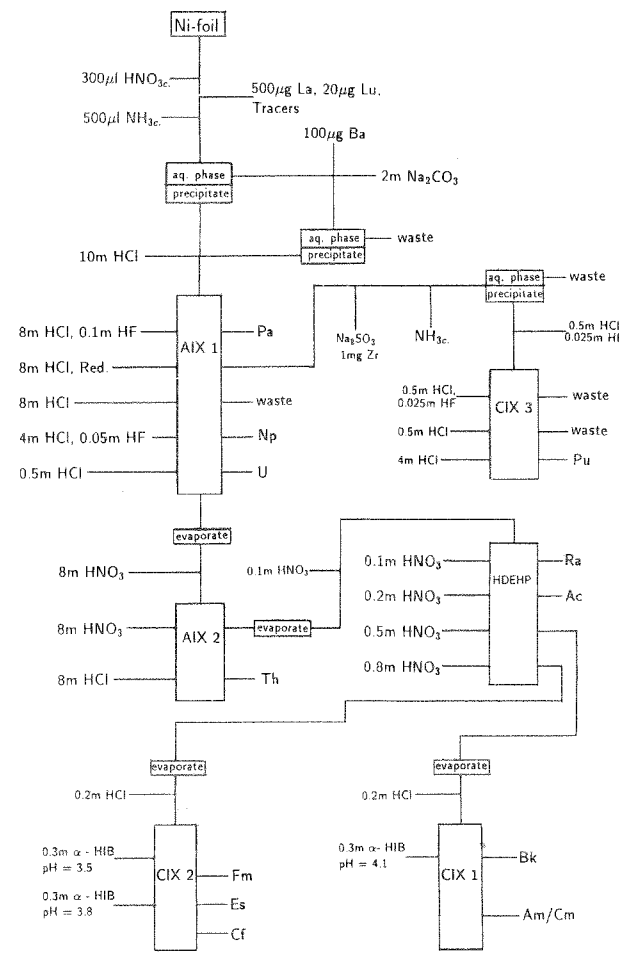

Fig. 1: Separation scheme for target-like reaction products

The Deposition of Polonium - A Comparison of Experimental and Calculated Yields

M. Schädel, B. Schausten, W. Brüchle
GSI Darmstadt

The yield of spontaneous deposition of polonium on silver has been studied[1] as a function of the volume of the solution, and of the time exposure from a hydrochloric acid solution. Fahland, Herrmann and Straßmann[2] have shown that the Nernst-Brunner equation[3]

$$y = a \times (1 - e^{-r \times t}) \qquad (1)$$

which describes the rate of diffusion through a solid-liquid interface, can also be applied to describe the deposition of carrier free isotopes. If necessary, the radioactive growth and decay have to be taken into account as an additional factor in Eq.(1). In the Nernst-Brunner equation the following terms are used:

t duration of the exposition
a number of atoms in the solution at t = 0
y number of atoms on the solid after the time t
F surface area of the exposed solid
V volume of the solution
D diffusion coefficient of the deposited material
i thickness of the interfacial film
k deposition constant
$r = k \times F/v$; $k = D/i$

From the Nernst-Brunner equation, the deposition constant, k, can be determined as:

$$k = \frac{V}{F \times t} \ln \frac{a}{a - y} \qquad (2)$$

These two equations have some nice features to check and plan experiments. The deposition constant, k, can easily be calculated for each individual experiment. Large deviations from a value which has previous by been determined for a specific reaction system and experimental set-up indicates an experimental problem. In a known system the yield of deposition can be calculated for any experimental time, and, if one has to account for radioactive decay, an optimum duration of the experiment can be calculated[2].

A comparison of calculated and experimentally determined yields of the deposition of polonium as a function of time, see Fig. 1, and volume, see Fig. 2, is given below. Details of experimental conditions of the Po deposition on silver from the buffered hydrochlorid acid solution are given in Ref. 1. The good agreement between the calculated and experimental values which can be observed from Figs 1 and 2 provides the confidence to apply the method to a search for Po on very low levels in solutions like laboratory reagents for example[4]. It has been shown that the concentration of the Po in the solution between 10^8 and 40 atoms does not influence the rate and yield of the deposition[5,6].

1. M. Schädel, B. Schausten, W. Brüchle, W. Weber, Scientific Report 1988, GSI 89-1 (1989) p. 265
2. J. Fahland, G. Herrmann, F. Straßmann, J. Inorg. Nucl. Chem. 7, 201 (1958)
3. E. Brunner, Z. Phys. Chem. 47, 56 (1904)
4. B. Schausten, M. Schädel, W. Brüchle, contribution to this annual report
5. F.-J. Reischmann, N. Trautmann, G. Herrmann, Radiochim. Acta 36, 139 (1984)
6. F.-J. Reischmann, B. Rumler, N. Trautmann, G. Herrmann, Radiochim. Acta 39, 185 (1986)

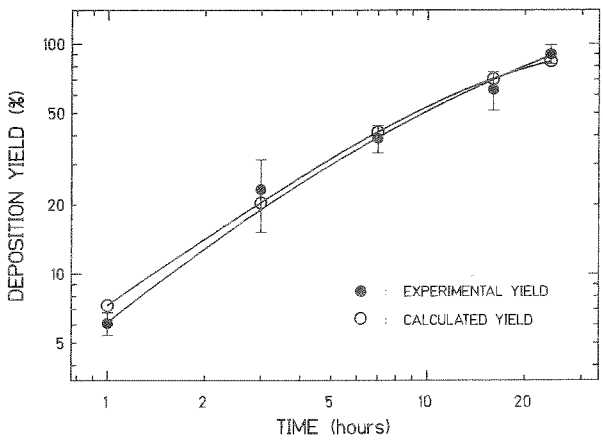

Fig.1:
Comparison of calculated and experimental deposition yields of Po as a function of the exposition time. The error bars represent one standard deviation.

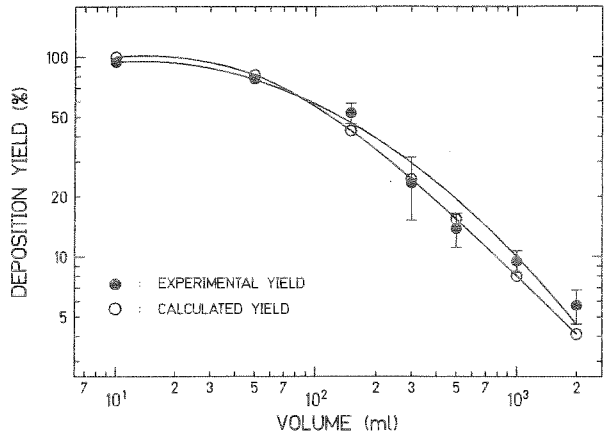

Fig.2:
Comparison of calculated and experimental deposition yields of Po as a function of the volume of the solution.

Deposition of Polonium from Hydrofluoric- and Phosphoric Acid

B. Schausten, W. Brüchle, M. Schädel
GSI Darmstadt

Our first studies to determine the deposition yield of polonium from hydrochloric acid[1] was motivated by the upcoming needs to determine small amounts of α-radioactive impurities in chemicals which are used to fabricate high density random access memories. The α-particle from the radioactive decay looses energy in the silicon and generates particle-hole pairs. As a result the bit state in the memory cell can be upset and altered, a so called soft error[2] occurs.

In producing semiconductors hydrofluoric- and phosphoric acid are commonly used reagents, and therefore we began to include these acids into our investigations. In this first step we again wanted to find out by using ^{210}Po tracer activities how applicable the method of spontaneous deposition from these acids is. To measure the deposition yields as a function of the volume of the solution and the exposure time have been the first goals of our investigation.

We have used the same procedure as described in the previous report[1] to buffer the acids and to prepare the solution for the polonium deposition on a silver plate. Slightly different absolute quantities of the various reagents have been used to adapt for the different acidities. The pH of the solution at the time of the beginning of the deposition, which is known to be an important parameter, was between 4.5 and 5. The solution was kept at boiling temperature under reflux conditions for the time of exposure. For the hydrofluoric acid a chemically inert Teflon destillation flask was used to avoid reaction with the glass walls.

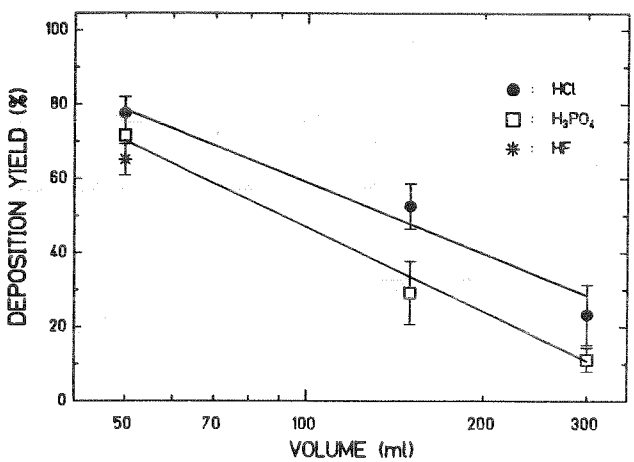

Fig. 1:
Yield of ^{210}Po deposition from hydrochloric- and phosphoric acid on silver as a function of volume. The curves represent fits to the data. The error bars of one standard deviation are given. One data point for hydrofluoric acid is shown at 50 ml.

The volume dependence of the deposition yield of the phosphoric acid in comparison with the data for hydrochloric acid is shown in Fig. 1 together with one data point for hydrofluoric acid. The plating time in all of these experiments was three hours. Because of instrumental limitations presently only one data point with a yield of 65% at a volume of 50 ml is available for the hydrofluoric acid. The deposition yield of polonium from hydrofluoric acid can be increased from 65% to 91% by increasing the plating time from three hours to seven hours. This is in good agreement with the time dependence observed for hydrochloric acid in earlier experiments. The yields are high and reproducible enough to use this method of spontaneous deposition of polonium on silver also for hydrofluoric- and phosphoric acid.

From our discussion of the Nernst-Brunner equation in a separate contribution to this report[3] we can expect to find different absolute yields for phosphoric acid, and also hydrofluoric acid, as compared with hydrochloric acid for a fixed time and volume. This is because of the presence of, most likely, different diffusion coefficients and thicknesses of the interface film at the solid-liquid interface. For the volume dependence of the deposition yields all acids should exhibit the same slope of a straight line in a semi-logarithmic presentation. Within the error bars this behaviour can be observed in Fig. 1 from a comparison of the hydrochloric- and phosphoric acid data. The result of the tracer studies with hydrofluoric- and phosphoric acid makes us confident that the spontaneous deposition of polonium on silver is a very useful method to determine small amounts of polonium impurities in these reagents.

1. M. Schädel, B. Schausten, W. Brüchle, GSI Scientific Report 1988, GSI 89-1 (1989) p. 265
2. T.C. May, M.H. Woods, 16th Ann. Proc. Reliability Physics 1978 (Symp. San Diego) 16, p. 33
3. M. Schädel, B. Schausten, W. Brüchle, contribution to this report

Polonium Content in Hydrochloric - and Hydrofluoric Acids

B. Schausten, W. Brüchle, M. Schädel
GSI Darmstadt

The search for trace amounts of polonium as a source of alpha radioactivity in laboratory reagents was stimulated by the discussion about soft errors [1] in high density random access memories.

The spontaneous deposition of polonium from buffered acid solutions on a silver foil is an establish method [2] for simultaneously separating the polonium and preparing a good sample for α-spectroscopy. From our parameter studies [3,4] and a comparison of experimental and calculated yields [5], we have determined conditions for a routine polonium deposition procedure.

The preparation of the solution is described in Ref. 3. For the hydrochloric acid we used a total volume of 300 ml and a deposition time of 24 hours at boiling point temperature. From the previous tracer experiments [3], we expect a deposition yield of 90% under these conditions. Because of the need to use a chemically inert Teflon apparatus with the hydrofluoric acid only a smaller total volume of 50 ml has been applied for this solution. With such a small volume a deposition yield of 91% can be obtained during an exposure time of seven hours [4]. The concentration of the initially applied hydrochloric - and hydrofluoric acid in this final plating solution was 12.3% and 16.0%, respectively. Each sample has been measured for 24 h with a Au(Si) surface barrier detector with a 36% efficiency. A typical spectrum of such a measurement is shown in Fig. 1.

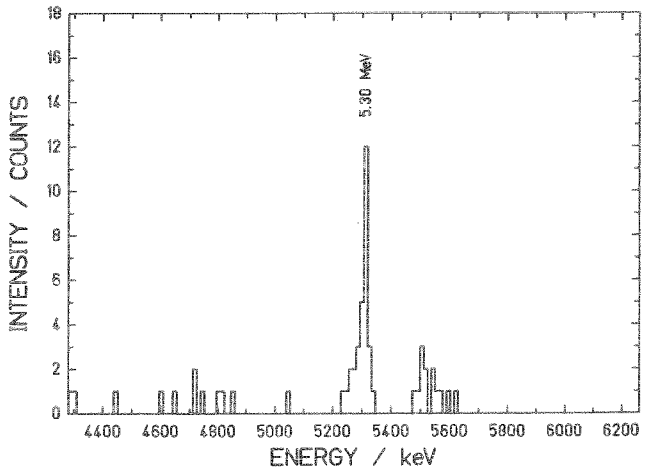

Fig. 1:
Alpha spectrum of ^{210}Po from a hydrofluoric acid solution. The observed activity corresponds to a polonium content of 2×10^{-18} mol/l in the solution.

Above the peak of ^{210}Po at 5.30 MeV with a total intensity of 30 counts a few events between 5.5 and 5,6 MeV from a calibration source can be seen. The background for this specific detector and counting chamber in the energy window 5.2 to 5.4 MeV, which has been used as integration limits for ^{210}Po, was three counts per day. A background of three alphas per day corresponds to a detection limit of about 1×10^{3} Bequerel ^{210}Po per liter or, in different units, 2.5×10^{-20} mol/l for a sample prepared from 300 ml hydrochloric acid solution.

We have started a series of first experiments to determine the ^{210}Po content in commercially available hydrochloric- and hydrofluoric acids of various concentrations and specified purities from various suppliers. The experiments are still in progress, and presently only first preliminary results can be reported.

Hydrochloric acids from three different companies with the specified purities 'technical pure', 'chemically pure', 'extra pure', 'Suprapur' and 'pro analysi' have been assayed. No significant differences, which means deviations of less than one order in magnitude, in the content of ^{210}Po were found in these solutions. On an average the observed activity in the hydrochloric acid has been about 1×10^{-2} Bq/l which corresponds to 3×10^{-19} mol/l. The ^{210}Po content in the hydrofluoric acid has been significantly higher. Again reagents from three different companies with similar specifications of the purities as for the hydrochloric acids has been investigated. The average observed activity was 1×10^{-1} Bq/l or 3×10^{-18} mol/l with an indication for slightly larger deviations of the polonium content between the individual solutions as compared with the hydrochloric acid.

1. T.C. May, M.H. Woods, 16th Ann. Proc. Reliability Physics 1978 (Symp. San Diego) 16, p.33
2. P.E. Figgins. The Radiochemistry of Polonium, NAS-NS 3037, 1961, p. 29
3. M. Schädel, B. Schausten, W. Brüchle, GSI Scientific Report 1988, GSI 89-1 (1989) p. 265
4. B. Schausten, W. Brüchle, M. Schädel, contribution to this report
5. M. Schädel, B. Schausten, W. Brüchle, contribution to this report

Gasphase chemistry experiments with element 105

D.T. Jost, H.W. Gäggeler, U. Baltensperger, Nai-qi Ya; *Paul Scherrer Institut, Villingen, Switzerland*
A. Türler, Ch. Lienert; *Institut für anorganische Chemie, Universität Bern, Switzerland*
K.E. Gregorich, C.M. Gannett, H.L. Hall, R.A. Henderson, D.M. Lee, J.D. Li, M.J. Nurmia, D.C. Hoffman; *LBL, Berkeley*
M. Schädel, W. Brüchle; *GSI Darmstadt*
J.V. Kratz, H.P. Zimmermann, U.W. Scherer; *Institut für Kernchemie, Universität Mainz*

Element 105 is (hahnium (Ha) or nilsbohrium (Ns) depending on the claim of its discovery) so far the heaviest element whose chemical properties have been investigated. Early work on the gas-phase chemistry by Zvara [1] indicated that it behaves similar to a group V element. We have investigated the formation and volatility of the $HaBr_5$ compound using on-line gaschromatography.

The experiments were performed with ^{262}Ha ($T_{1/2}$=35s), produced in the reaction $^{249}Bk(^{18}O,5n)$ at the 88"-cyclotron at LBL. The gas-jet technique and a gaschromatography set-up similar to the one used in previous experiments [2,3] were employed. The LBL MG-wheel counting device with an 18 second stepping time was used to detect alpha- and fission- events. Pairs of CANBERRA PIPS (passivated ionimplanted planar silicon) detectors were installed in 6 counting positions giving a total counting time of 108 s after the end of the collection. These PIPS detectors proved to be very resistant to the corrosive gases used. Spectroscopic data was recorded event by event. An analysis of all data accumulated in runs using HBr/BBr_3 and temperatures from 300 to 500 ^{0}C give for the alpha events in the energy region of ^{262}Ha and its daughter ^{258}Lr (8.35-8.75 Mev) a half-live of 33±6 s, in good agreement with the literature. Low energy tailing from the neighboring ^{211m}Po at 8.88 Mev contributes less than 40 % giving a lower limit of 160 ^{262}Ha events.

The bromide complexes were formed by adding HBr or HBr which had passed over BBr_3 to the carrier gas at the entrance of the gaschromatograph. Figure 1 shows the chemical yield curves for the Ha and its homologous elements Nb and Ta as a function of temperature. From these curves we conclude that $HaBr_5$ is more volatile than the corresponding tantalum compound since the maximum yield is found at a lower temperature and that $NbBr_5$ is more stable than $HaBr_5$ since it can be formed without adding BBr_3 to the HBr. These findings are in contrast to the volatility sequence Nb>Ta>Ha recently published by Timochin et al. [4] who used HBr/Br_2 but in agreement with Kratz et al. [6] who showed that in aqueous solutions the hahniumhalide complexes are more like the Nb complexes than the Ta ones.

Figure 2 shows the decay analysis of the fission activity of direct catch experiments (no chemistry). A new, so far not identified fission activity with a half live of 14±4 s is clearly visible above the background from the spontaneous fission activity of long lived actinides. This same activity was also found in runs where HBr/BBr_3 was used as bromating agent whereas in runs with HBr alone it was not seen. This suggestes an origin with a similar bromide chemistry as Ha. A fission activity with the 35 s half-live of ^{262}Ha could not be identified.

According to Gregorich et al. [5] ^{262}Ha has a 50% spontaneous fission branch. Taking the above sum of 160 ^{262}Ha events an equal number of sf-events decaying with a 35s half-live should have been seen. Comparing this with 19 events observed in the first 60 seconds we find that the sf-branch is less than 25%.

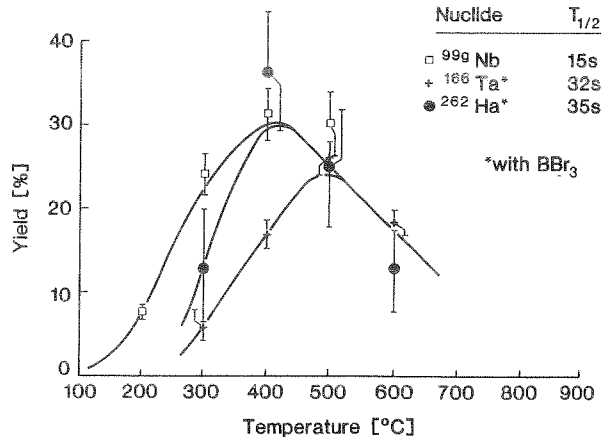

Fig.1: Chemical yields for group V elements Nb, Ta and Ha

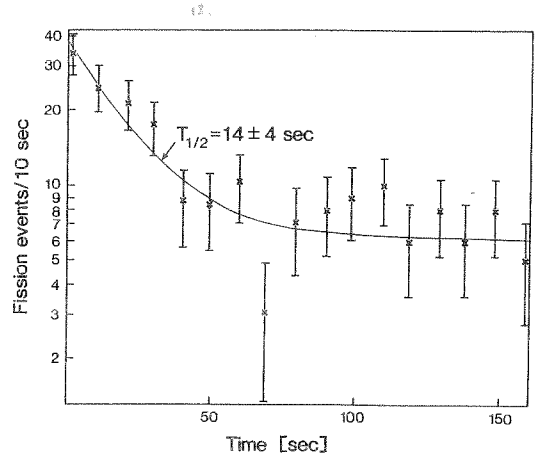

Fig.2: Decay analysis of sf-events in a direct catch experiment with 36s stepping time.

[1] I. Zvara et al., Sov. Radiochem. **18**,328(1976)
[2] D.T. Jost et al., Inorg. Chim. Acta **146**,255(1988)
[3] Nai-Qi Ya et al., Radiochim. Acta, **47**,1(1989)
[4] S.N. Timochin et al., Abstract Int. School Seminar on Heavy Ion Physics, Dubna, Oct. 3-12(1989),p. 20
[5] K. Gregorich et al., Radiochim. Acta, **43**,233(1988)
[6] J.V. Kratz et al., Radiochim. Acta **48**,121(1989)

Elution of Lanthanides and Actinides with α-Hydroxy-Isobutyrate from Cation Exchange Columns Revisited

M. K. Gober[1], J. V. Kratz[1], U. W. Scherer[2]

[1]Institut für Kernchemie der Universität Mainz, [2] presently at Paul Scherrer-Institut, CH-5303 Würenlingen

For ions of the same charge and hydration number in a given chromatographic system the logarithm of the distribution coefficient, $logK_D$, is a linear function of the ionic radius [1]. This linear correlation is expected to break down when the hydration (coordination) number CN is changed. From the measurement of diffusion coefficients for several Ln^{3+} and An^{3+} ions at 25°C it is known [2] that a change of CN from 8 to 9 occurs around Eu^{3+} in the lanthanide series and around Bk^{3+} in the actinide series with the smaller value of CN being associated with the heavier elements in both series. For higher temperatures measurements of CN are not available, and it was argued [3] that the discontinuity might then occur at lower atomic number. This should cause a temperature-dependent discontinuity in the correlation of $logK_D$ *vs.* ionic radius also in α-HIB/CIX separations. The published K_D-values for 87°C [4] and for 25°C [5] are not necessarily compatible with this proposition. Therefore, we have considered it worthwhile to remeasure systematically the elution positions of Ln^{3+} and An^{3+} ions from CIX columns with α-HIB solutions at both room temperature and 87°C.

Lanthanide tracer activities and actinides were either produced by reactor irradiations, obtained commercially, or were produced by heavy-ion bombardements. Mixtures of the tracers were dissolved in ~100μl of a 0.025M α-HIB solution and were added to our standard HPLC system through a sample loop and absorbed on top of a 2×60mm column packed with Aminex A6 cation exchange resin (particle size 17.5 ± 2μm) kept at 25°C or 87°C, respectively. They were subsequently eluted from the column with α-HIB solution. Concentration and pH of the α-HIB solutions were varied, because elution of all Ln^{3+} and An^{3+} ions with the same α-HIB would lead to poor separation of the heavy elements and unreasonably long times for eluting the lighter elements, which would elute in very broad peaks. So the lanthanides and actinides were divided in groups of up to eight elements, each group being eluted at an optimum concentration and pH of the α-HIB. The effluent was assayed for γ- and α-activity in order to determine the distribution of the lanthanide and actinide tracer activities. From the retention volumes associated with the peak maxima of the elution curves the logarithm of the distribution coefficients, $logK_D$, were determined as a function of the ionic radius [6].

As shown in fig.1, for 25°C $logK_D$ is a function of the ionic radius *and* of the negative logarithm of the α-HIB-concentration, pL. The resulting plain has a discontinuity caused by the change of CN and is twisted because the slope of the function $logK_D$ *vs.* r_{ion} is dependent on the pL. The position of the discontinuity also varies: with rising α-HIB concentration it is drifting towards bigger ionic radii. At 87°C the situation is similar (fig.2), but the break in the linear correlation of $logK_D$ *vs.* r_{ion} seems to occur at smaller ionic radii. This explains why the comparision of elution data for the two temperatures obtained at different pL's as in [7] is misleading because here the discontinuity occurs in the same range of ionic radii only by chance [8].

Figure 1

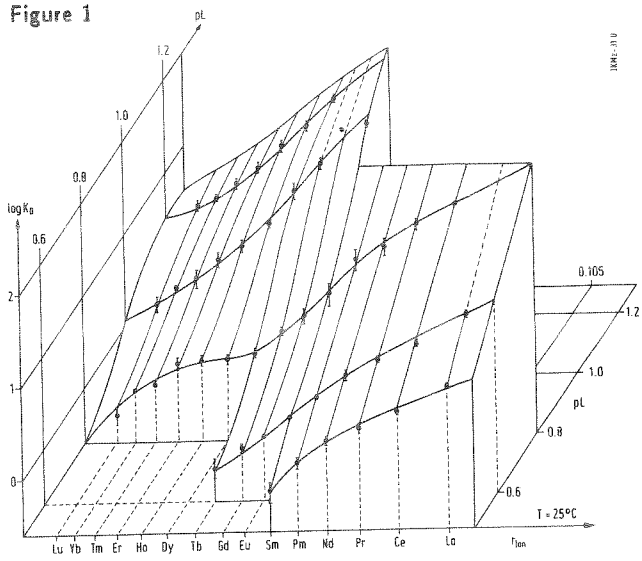

Figure 2

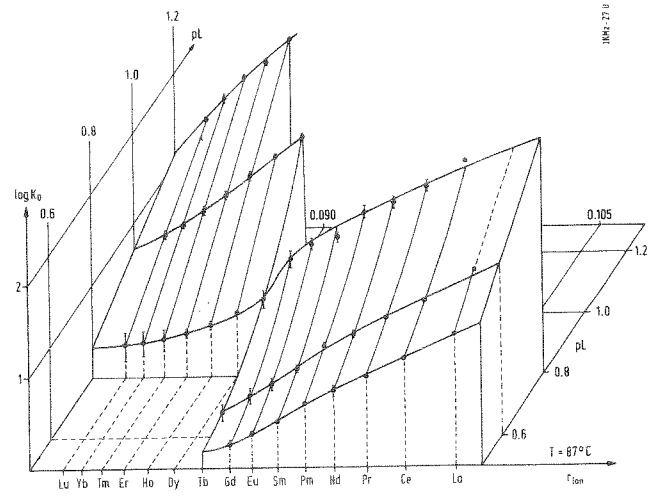

References

[1] Y. Marcus, A.S. Kertes, Ion Exchange and Solvent Extraction of Metal Complexes, Wiley,1969, p. 287

[2] F. David, J. of the Less Common Metals 121,27 (1986)

[3] F. David, private communication

[4] G. H. Higgins, 'The Radiochemistry of the Transcurium Elements', U.S. NAS-NS-3031,1960

[5] H.L. Smith, D.C. Hoffman, J. Inorg. Nucl. Chem., 3, 243 (1956)

[6] D. H. Templeton, C. H. Dauben, JACS 76, 5237 (1954)

[7] M.K. Gober, J.V. Kratz, U.W. Scherer, GSI-Jahresbericht 1988

[8] M.K. Gober, Diplomarbeit, Mainz 1989, p. 51

USCHI Trimmed for HDMP

E. Schimpf, E. Jäger, K.H. Behr, M. Schädel
GSI Darmstadt

The scattering chamber USCHI, previously used for Rutherford back scattering experiments[1] in the UNILAC stripperhall has been trimmed for its installation as a manifold usable vacuum chamber for various types of experiments at the high dose multipurpose cave (HDMP) at SIS. Precautions where not only taken to provide a universal and easily accessible chamber for many kinds of irradiation and activation experiments with high beam intensities up to the design value of SIS, but also to furnish a well suited environment for test of detectors, and last, but not least, to investigate such kind of rare reaction channels in nuclear physics experiments in which the use of the highest available beam intensities are a prerequisite. USCHI will be installed at a position 16m downstream the first quadrupole triplett of the FRS in front of the SIS beam dump.

A cross section through the rebuilt chamber and some of the new peripheral parts is shown in Fig. 1. The beam enters and exists the chamber through short beam pipes mounted inside the chamber, see Fig. 2., which optionally can be equipped with beam windows to also allow for irradiations in an atmosphere different from the 'standard' vacuum of $< 1 \times 10^{-6}$ Torr obtained with two turbo molecular pumps (TPU 1500 and TPU 510). A piece of beam pipe to connect, if desired, the open ends inside the chamber is available. The beam traverses the chamber at a height of 312 mm above a removable platform on which the experimental set-up can be mounted. The available height above the beam is 400 mm to the rim of the tank, and additional 400 mm in the middle of the lid. While the inner horizontal diameter of the chamber is 1.5 m the removable platform provides an easy access for set-ups smaller than 850 mm in diameter. An opening of 250×200 mm² in the middle of the platform allows to insert targets and/or detectors through a NW 250 gate value from underneath into the chamber. This gate valves separated the big vacuum tank from a smaller sluice chamber with the inner dimensions of $430 \times 300 \times 300$ mm³ which can be pumped separately. Experimental set-ups of up to 40 kg, can be mounted on a combination of a tilt platform and a translation stage for a precise adjustment ($< 10\mu$m) in the irradiation position. A stepping motor in combination with a shaft decoder provides the vertical movement between the two chambers and the vertical position adjustment.

Two out of six large flanches (400×300 mm²) which are accessible on the chamber furnish 96 electrical (BNC) and 16 gas feed through at present. In addition, a variety of smaller flanches may be used. The chamber will house additional elements for the diagnostics of the size and the position of the beam close to the target.

1. M. Brügger, K. Lützenkirchen, S. Polikanov, G. Herrmann, M. Overbeck, N. Trautmann, A. Breskin, R. Chechik, Z. Fraenkel, and U. Smilansky, Nature 337, 434 (1989)

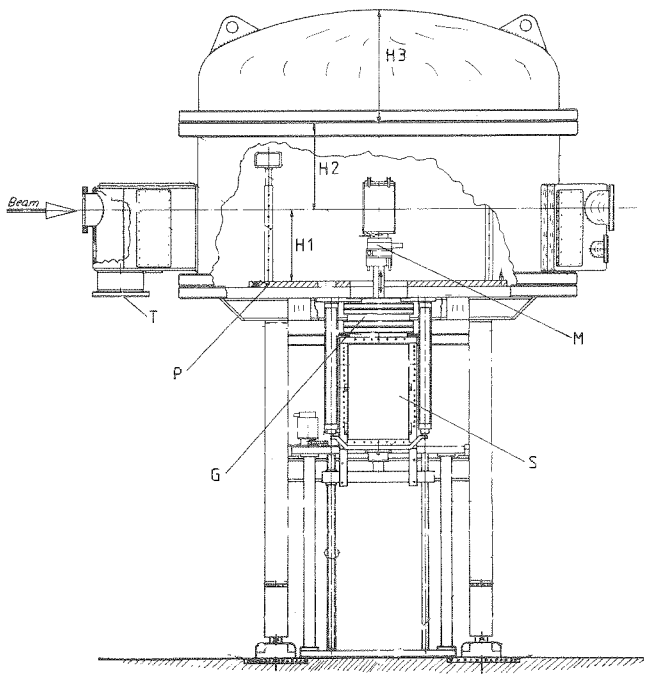

Fig.1: Schematic side view of USCHI.
G = gate valve NW 250, M = translation stage and tilt platform, P = removable platform, S = sluice chamber, T = turbomolecular pump TPU 1500, H1 = 312 mm, H2 = 400 mm, H3 = 400 mm.

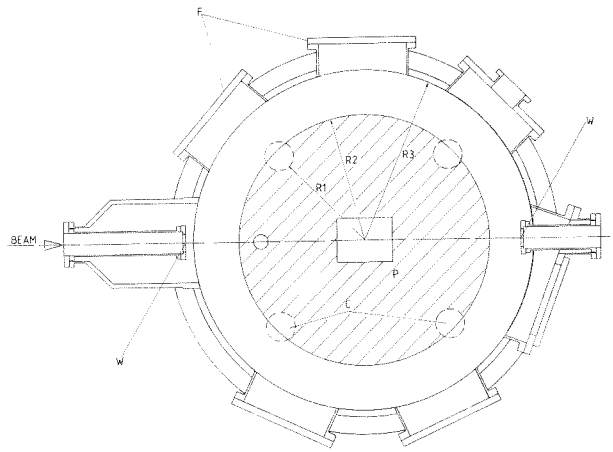

Fig.2: Schematic top view of USCHI.
W = inner beam pipes with NW 100 or beam window, F = large flanches, C = poles to carry the platform with a crane, R1 = 480 mm, R2 = 570 mm, R3 = 750 mm, P = removable platform.

Determination of Trace Amounts of Platinum in Glasses using Rutherford Backscattering

E.Stiel[b], G.Herrmann[b], J.V.Kratz[b], K.Lützenkirchen[b], M.Overbeck[b], S.Polikanov[a], C.Sastri[a], and N.Trautmann[b]

[a] Gesellschaft für Schwerionenforschung mbH, Darmstadt

[b] Institut für Kernchemie, Universität Mainz

Nuclear backscattering has become a valuable tool to analyze samples composed of light to medium mass elements. It is usually performed by using α–particles as projectiles which are backscattered from target samples due to Coulomb repulsion and whose energy after scattering is measured with semiconductor detectors. The energy after scattering E' is related to the initial energy E_o through

$$\frac{E'}{E_o} = \frac{m \cdot cos\theta + \sqrt{M^2 + m^2 \cdot sin^2\theta}}{m + M} \qquad (1)$$

with m and M as projectile and target masses in amu and θ as scattering angle. Thus, by measuring E' one can deduce the mass number of the target atom. The RBS method can also be used for quantitative analyses with accuracies usually in the percent range.

Recently, the problem was raised to determine concentrations of platinum in glasses on the ppm–level. If the platinum concentration increases above a certain value in the ppm–range, the platinum atoms start to form larger aggregates which deteriorates the optical properties of the glass. We decided to test the applicability of RBS for this problem, however, by applying a kind of particle detection more sophisticated than the usual semiconductor–based one, see below.

Another major difference between our experiment and a more traditional RBS experiment is the use of ^{40}Ar–ions as projectiles instead of the usual α–particles. This is quite essential for the determination of platinum, since other heavy elements might be present in the sample. The difference in energy loss of α–particles backscattered from platinum (A=198) on the one hand and from nuclei in the A=100–150 mass region on the other is too small to be reasonably well resolved. This situation improves for heavier projectiles (see eq.1).

As detection device we used the heavy–ion identification system installed at GSI's stripper hall initially set up to search for "strange matter" [1]. The present study was performed by using ion beams from the UNILAC with an energy of 1.4 MeV/u. Scattered nuclei were detected in a system of twelve low-pressure multiwire proportional counters [2] divided into four identical modules each of which consisted of one start and two stop detectors. The ranges of scattering angles covered by this system are 92°–120° and 127°–170° with a total solid angle of 1.15 sr. Detected nuclei are identified by measuring the time-of-flight (TOF) and the specific ionization (ΔE). The scattering angle is obtained from the position measurements in start- and stop-detectors.

In our experiment a glas target with a known platinum concentration of 5 ppm was irradiated. As another heavy element the glas contained 1-3% of barium. The irradiation lasted about one hour with a total of $1.3 \cdot 10^{13}$ projectiles of ^{40}Ar.

In Figure 1 data of part of a detector module are displayed. The TOF of ^{40}Ar is depicted as a function of the laboratory scattering angle θ. One can clearly distinguish two different groups in the figure. The first one is in the range TOF = 45 – 55 ns, the second one in the range TOF = 55 – 80 ns. The solid line is deduced from calculated values corresponding to ^{40}Ar backscattered from ^{195}Pt, the dashed line corresponds to ^{40}Ar backscattered from ^{138}Ba. The bulk of the glas does not contribute to backscattering of ^{40}Ar, since it consists largely of the lighter elements silicon and oxygen.

The sum of all events of Figure 1 corresponding to scattering from ^{195}Pt is 179; in the whole system 1015 events were detected. We assume that in order to identify platinum about 50 events would have been sufficient. Thus, the detection limit in our experiment is 0.3 ppm. By using larger projectile doses even lower concentrations can of course be determined.

References

[1] M.Brügger et al. Nature(London) *337* (1989) 434.

[2] M.Overbeck et al. Nucl. Instr. and Meth., in press.

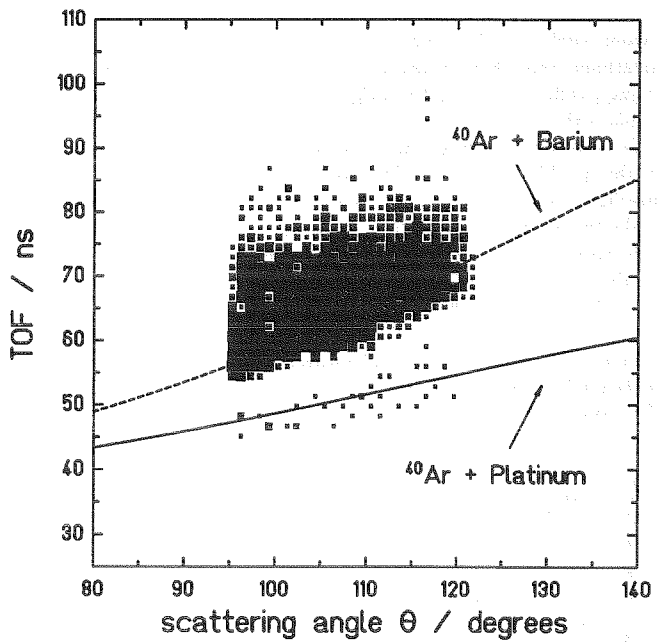

Fig.1: Two - dimensional representation of the time-of-flight of ^{40}Ar–particles backscattered from a glas containing barium and platinum as a function of the laboratory scattering angle θ.
Solid line: Calculated values for ^{40}Ar backscattered from platinum
Dashed line: Calculated values for ^{40}Ar backscattered from barium